



Published in final edited form as:

*Clin J Pain.* 2017 December ; 33(12): 1071–1080. doi:10.1097/AJP.0000000000000509.

## PPAR $\gamma$ AGONISTS ATTENUATE TRIGEMINAL NEUROPATHIC PAIN

Danielle N. Lyons<sup>1</sup>, Liping Zhang<sup>1</sup>, Robert J. Danaher<sup>2</sup>, Craig S. Miller<sup>2</sup>, and Karin N. Westlund<sup>1</sup>

<sup>1</sup>Department of Physiology, University of Kentucky, Lexington, Kentucky 40536-0298

<sup>2</sup>Department of Oral Health Practice, University of Kentucky, Lexington, Kentucky 40536-0298

### Abstract

The aim of this study is to investigate the role of peroxisome proliferator-activated receptor-gamma isoform (PPAR $\gamma$ ), in trigeminal neuropathic pain utilizing a novel mouse trigeminal inflammatory compression (TIC) injury model. The study determined that the PPAR $\gamma$  nuclear receptor plays a significant role in trigeminal nociception transmission, evidenced by: **1)** Intense PPAR $\gamma$  immunoreactivity is expressed 3 weeks after TIC nerve injury in the spinal trigeminal nucleus caudalis (spV), the termination site of trigeminal nociceptive nerve fibers. **2)** Systemic administration of a PPAR $\gamma$  agonist, pioglitazone (PIO), attenuates whisker pad mechanical allodynia at doses of 300 mg/kg i.p. and 600 mg/kg p.o. **3)** Administration of a PPAR $\gamma$  antagonist, GW9662 (30 mg/kg i.p.), prior to providing the optimal dose of PIO (300 mg/kg i.p.) blocked the analgesic effect of PIO. This is the first study localizing PPAR $\gamma$  immunoreactivity throughout the brainstem trigeminal spinal trigeminal nucleus caudalis (spV) and its increase three weeks after TIC nerve injury. This is also the first study to demonstrate that activation of PPAR $\gamma$  attenuates trigeminal hypersensitivity in the mouse TIC nerve injury model. The findings presented here suggest the possibility of utilizing the FDA approved diabetic treatment drug, PIO, as a new therapeutic that targets PPAR $\gamma$  for treatment of patients suffering from orofacial neuropathic pain.

### Keywords

Trigeminal Inflammatory Compression (TIC) injury; PPAR $\gamma$ ; spV; mice; mechanical threshold; immunoreactivity

### Introduction

Trigeminal neuropathic pain is an orofacial pain condition characterized by continuous aching and burning sensation caused by trigeminal nerve damage<sup>1</sup>. Dental procedures or trauma can cause trigeminal peripheral nerve injury and inflammation, but in some cases, the cause is unknown. Clinicians most often treat this continuous trigeminal neuropathic pain with anticonvulsants and antidepressants, alone or in combination, which yields

variable treatment responses<sup>2-5</sup>. Therefore, there is a great need for discovery of new drug targets.

The goal of the present studies was to investigate the potential for utilizing the clinically used thiazolidinedione pioglitazone, which reportedly decreases microglial activation and certain cytokines such as tumor necrosis factor alpha (TNF- $\alpha$ ) and Interleukin 6 (IL-6)<sup>6, 7</sup>. Thiazolidinediones target peroxisome proliferator-activated receptor (PPAR). PPAR is a nuclear receptor with three isoforms: alpha, beta/delta and gamma<sup>8</sup>. PPAR is widely expressed in adipose, liver, cardiac, endometrial stromal cells, immune cells, neurons, and glia of the peripheral and central nervous system<sup>9-17</sup>. After ligand-activation, the PPAR transcription factors of the nuclear hormone receptor superfamily play a major regulatory role in energy homeostasis and metabolic function<sup>18</sup>. These receptors form a heterodimer with retinoid X receptor (RXR) controlling gene expression of PPAR response elements on DNA<sup>8, 19-21</sup>. In particular, the activation of PPAR $\gamma$  has been shown to have multiple downstream effects.

PPAR $\gamma$  is activated by endogenous lipids or by thiazolidinediones, such as rosiglitazone and pioglitazone (PIO), which are FDA approved for the treatment of type 2 diabetes. These agonists have been shown to regulate fatty acid metabolism<sup>19, 22, 23</sup>. However, more recent studies suggest PPAR $\gamma$  activation plays a role in another major pathway that suppresses neuro-inflammatory mediators, such as NF- $\kappa$ B (nuclear factor kappa-light-chain-enhancer of activated B cells), thereby decreasing microglial activation, as well as TNF- $\alpha$  and IL-6<sup>6-8, 24</sup>. In addition to a reduction in paw edema after capsaicin injection, PPAR $\gamma$  activation also reduces mechanical allodynia and thermal hyperalgesia in the sciatic nerve injury animal models<sup>6, 15, 25-28</sup>. Furthermore, PPAR $\gamma$  has been shown to be upregulated in Schwann cells after nerve injury<sup>29, 30</sup>. Other studies have found that PPAR $\gamma$  in the retina is upregulated within 3 days after an optic nerve injury in a mouse and then returns to basal levels by day 14<sup>31</sup>.

Although PPAR $\gamma$  activation clearly is implicated in a decrease of specific types of neuropathic and inflammatory pain, the effects of PPAR $\gamma$  activation on trigeminal pain have not been studied. While Moreno et al. reported evidence of PPAR in the trigeminal nucleus<sup>32</sup>, no one has explored the function of this receptor in the brainstem spinal trigeminal (spV)<sup>3, 33</sup>. The spV consists of trigeminal nociceptive sensory nerve primary endings and second order system neurons that send information about painful stimulation to the thalamus via the trigeminothalamic pathway which then transmits the signals to the head/neck/facial region of the sensory cortex (layer IV)<sup>3, 33, 34</sup>.

The aim of this study is to determine the role of PPAR $\gamma$  in trigeminal neuropathic pain utilizing our novel mouse trigeminal inflammatory compression (TIC) injury model<sup>35</sup>. Our findings are that 1) the immunoreactivity for PPAR $\gamma$  is increased in spVc at 3 weeks in mice with TIC injury and 2) PIO attenuates trigeminal TIC nerve injury related pain dependent on PPAR $\gamma$  activation. We evaluated: 1) PPAR $\gamma$  immunoreactivity in the spV with/without TIC injury, 2) systemic administration of PIO, PPAR $\gamma$  agonist, in mice with TIC injury to assess the attenuation of trigeminal neuropathic pain, and 3) systemic administration of PPAR $\gamma$

antagonists to better determine whether PIO acts through PPAR $\gamma$  dependent pathways to attenuate orofacial neuropathic pain.

## Materials and Methods

All experimental procedures were performed in accordance with the guidelines provided by the National Institute of Health (NIH) regarding the care and use of animals for experimental procedures. Animal protocols were approved by the University of Kentucky's Institutional Animal Care and Use Committee (IACUC). All animals were housed in facilities approved by the Association for Assessment and Accreditation of Laboratory Animal Care International (AAALAC) and the United States Department of Agriculture (USDA).

## Animals

All experiments were performed with C57Bl/6 male, wild-type mice that weighed between 25 and 35 grams (g) purchased from Harlan Laboratories (Indianapolis, IN). Animals were randomly assigned to receive either experimental (TIC injury model) surgical procedures, sham surgical procedures, or to remain in the naïve cohort. Mice were housed in a well-ventilated mouse housing room (maintained at 20 – 22 °C) with a reversed 10/14 h dark/light cycle so that testing could be performed in their active period. All mice had access to food and water ad libitum throughout the duration of the experiment. Low soybean content normal chow diet was provided (Teklab 8626, Harlan, Indiana).

## Trigeminal Inflammatory Compression (TIC) Surgery

Mice were anesthetized with sodium pentobarbital (70 mg/kg, i.p.). With standard sterile surgery, the head was shaved, and ophthalmic cream applied over the eyes to protect them from over-drying. Mice were then fully constrained in a stereotaxic frame. A small 15 mm incision was made along the midline of the head and the conjunctiva of the orbit was opened along the top inner corner of the left eye bony socket with the tip of the surgical scalpel blade. Small cotton balls were used as tools in the orbital cavity for blunt tissue isolation and bleeding control. The infraorbital nerve was located approximately 5 mm deep against the maxillary bony infraorbital fissure in the orbital cavity. Animals randomly assigned to receive the TIC surgery underwent surgical placement of a 2 mm length of chromic gut suture (6-0), inserted between the infraorbital nerve and the maxillary bone infraorbital fissure. Chromic gut suture was inserted specifically in this region to adhere to specific infraorbital nerve bundles in order to prevent the chromic gut suture from sliding into the orbital cavity, but not to pierce the entire infraorbital nerve. Mechanical allodynia was induced in the mouse whisker pad ipsilateral to the surgery side due to the physical stimulation provided by the chromic gut suture against the nerve as well as the chromate salt released from the suture. Animals assigned to receive sham surgical procedures did not have the chromic gut suture placement, but only received the skin incision. Naïve animals did not receive any surgery. All mice were aged matched.

## Detecting Mechanical Allodynia on the Whisker Pad with the von Frey Fiber Test

Mechanical threshold of the whisker pad was measured before and after surgery with a modified up/down method (Chaplan et al., 1994) using a graded series of von Frey fiber filaments (force: 0.008 g (size: 1.65); 0.02 g (2.36); 0.07 g (2.83); 0.16 g (3.22); 0.4 g (3.61); 1.0 g (4.08); 2.0 g (4.31); 6.0 g (4.74); Stoelting, Wood Dale, IL). One experimenter gently restrained the mouse in their palm (2–5 minutes) with a cotton glove until the mouse was acclimated and calm. A second experimenter applied the von Frey filaments to the mouse's whisker pad. The 0.16 g (3.22) fiber was applied first. If the mouse responded three or more times out of five trials to the fiber, this was considered to be a positive response and the next lower gram force filament was applied. However, if the mouse responded two or fewer times out of five to the fiber applied, this was recorded as a negative response and then the filament with the next higher gram force was applied. Head withdrawal/front paw sweeping/biting behaviors were considered positive responses. Time between applications of each filament was 2–10 seconds. After one fiber successfully caused positive responses, application of the subsequent fibers continued until four fibers were applied or until the threshold was established positive response to the lowest gram force fiber. Data were analyzed with a curve-fitting algorithm that allowed for estimation of the 50% mechanical withdrawal threshold (measured in gram force). The decreased mechanical threshold value is an index of mechanical allodynia. Responses to the von Frey fiber stimulations were recorded on day 7 post surgery (TIC and sham) and continued once a week post-surgery, testing both the ipsilateral and contralateral whisker pads. A cohort of naïve mice was tested intermittently (weeks 2, 4, 8, 10, 11) alongside the sham animals and mice with TIC.

## Immunohistological Study

Mice with TIC injury, 3 weeks post injury, and aged matched naïve mice were anesthetized with isoflurane and perfused transcardially with heparinized saline followed by 4% ice-cold paraformaldehyde in 0.1 M phosphate buffer solution (PB, pH 7.4).

The brainstem was dissected and then placed in 4% paraformaldehyde in 0.1 M phosphate buffer solution (PB, pH 7.4) for overnight post fixation. This was followed by a 24 hour soak in 30% sucrose in PB. The brainstems were then embedded in OCT Compound (Tissue-Tek, Sakura, Torrance, CA) and sectioned with a cryostat at the thickness of 40 microns which were placed sequentially in 24-well plates filled with Ethylene Glycol based anti-freeze solution, stored at  $-20^{\circ}\text{C}$  until immunohistological study. To insure the integrity of the stain and control for variability, tissue sections (9–12/each animal) from different groups were simultaneously processed on the same day. On the day of immunostaining, the tissue sections were floated to wash with 0.1M PBS (pH 7.4), and pretreatment with 3% hydrogen peroxide in 0.1M PBS (pH 7.4) for 15 min to destroy endogenous peroxidase activity in erythrocytes. Tissue sections were then blocked using 0.5% Triton X-100 in PBS (15 min) to permeabilize cell membranes and reduce cell surface tension to increase the antibody penetration. Subsequent 5% normal goat serum in PBS (40min) was used to block nonspecific antigen-antibody combinations. Sections were incubated overnight at  $4^{\circ}\text{C}$  with rabbit polyclonal anti-PPAR-gamma IgG (1<sup>st</sup>. antibody) (1:6000 dilutions; H-100 Santa Cruz Biotechnology, Dallas, TX). The subsequent day, the sections were processed with a ABC Kit (Vectastain ABC Kit, Vector Laboratories, Inc. Burlingame, CA) i.e. incubated at room

temperature with a secondary bioatinylated goat anti-rabbit IgG (1:200) for 40 minutes. The sections were then incubated with avidin-biotin complex (ABC) reagent for 40 minutes. Finally, the antibody-antigen interaction was visualized with a peroxidase-catalyzed reaction. The sections were mounted onto Superfrost Plus glass slides which are electrostatic to attract frozen tissue sections (VWR MicroSlides, VWR International, LLC, Radnor, PA). The slides were allowed to air dry for at least 4 hours before they were dehydrated through graded ethanol and xylene. The slides were then cover-slipped using Permount mounting medium (Fisher Scientific, Waltham, MA). The slides were imaged using Nikon E1000 microscope (Nikon Instruments, Inc., Melville, NY) equipped with a Nikon DXM1200F digital camera and the Act-1 Program.

### Image Analysis

The immunostaining intensity within the brainstem trigeminal sensory spV nucleus subnuclei (oralis, interpolaris, and caudalis) was analyzed from the digitized images (9–12 tissue sections/animal, n=3) spaced at 400  $\mu\text{m}$  intervals using ImageJ (1.46, NIH). Each subnucleus of the spV was identified as a region of interest and analyzed for mean fluorescent intensities. To identify PPAR $\gamma$  immunoreactivity differences, each subnucleus of the complex was analyzed separately. The mean fluorescent intensities of the spV dorsal horn were measured in mice with TIC injury and then compared to that in naïve mice.

### Drug Preparation and Administration

Several PPAR agonists and antagonists were tested. (See Table 1 for drug administration, doses, and actions.) The PPAR $\gamma$  agonist, pioglitazone hydrochloride (PIO, Santa Cruz Biotechnology, Inc, Dallas, Texas) was dissolved in normal saline followed by 30 seconds of vortexing. Then the solution was sonicated for 20 minutes before use. A PPAR $\alpha$  agonist, Bezafibrate (2-[4-[2-(4-Chlorobenzamidoethyl)]phenoxy]-2-methylpropanoic acid, Sigma-Aldrich, St. Louis, MO), was dissolved in 1% carboxymethylcellulose and was vortexed for 30 seconds. Fenofibrate, PPAR $\alpha$  agonist; GW0742, PPAR $\beta/\delta$  agonist and GW9662, PPAR $\gamma$  antagonist (Cayman Chemical Company, Ann Arbor, Michigan) were dissolved in 10% dimethyl sulfoxide (DMSO, Sigma, St. Louis, MO) in saline and vortexed for 30 seconds before administration. All drugs were fresh prepared on the day just before administration.

Drugs were administered at least 8 weeks post operation after mechanical allodynia was confirmed to determine the efficacy of each drug in the chronic neuropathic pain condition. All doses were chosen based on drug safety and efficacy reported in previous studies<sup>6, 25, 27, 28, 36–40</sup>. Pioglitazone was administered intraperitoneally (i.p.) at doses of 100 mg/kg and 300 mg/kg (<10ml/kg volume) with a 30G/3/10cc sterile insulin syringe (BD, Franklin Lakes, NJ). Lower doses of pioglitazone ( 100 mg/kg) have been reported in previous studies, but when no effect was observed at 100 mg/kg, doses were increased accordingly. For a mouse, the reported LD50 of PIO given systemically ranges from 181–1200 mg/kg, therefore the 600 mg/kg dose has been administered orally (United States Pharmacopeial Convention, 2013). Oral gavage of 600 mg/kg was administered in a volume of <10 ml/kg with a stainless steel curved oral gavage needle (22  $\times$  1.5mm tip, Med-Vet International, Mettawa, IL)<sup>41</sup>.

The PPAR $\alpha$  agonists, Bezafibrate (100 mg/kg p.o.; LD50 500 mg/kg) and fenofibrate (200 mg/kg i.p.; LD50 1200 mg/kg), and the PPAR $\beta/\delta$  agonist, GW0742 (1 mg/kg and/or 6 mg/kg i.p.) were given systemically to serve as PPAR activation controls. The LD50 of GW0742 has not been reported.

In a separate cohort of mice, the PPAR $\gamma$  antagonist, GW9662 (30 mg/kg i.p.), was injected 30 minutes before the PPAR $\gamma$  agonist, pioglitazone (300 mg/kg i.p.) was given. This dose of PIO was chosen because it had the maximum effect on the elevation of mechanical threshold in TIC injury animals in our dose response study. GW9662 was used to block PIO from binding to PPAR $\gamma$  as in previous studies<sup>6, 38, 42</sup>.

During each drug testing, mechanical threshold was measured at time points of 0, 0.5, 1, 2, 3, 4 hours post treatment on the ipsilateral whisker pad only. The 600 mg/kg oral dosing of PIO was tested for 6 hours because an attenuation effect was observed starting at the 4<sup>th</sup> hour post injection time point. To increase in the animal “n” numbers in the treatment groups for these experiments, mice were tested with these drugs using the Latin square type crossover method with at least 1 week interval between each drug testing to allow sufficient time for the effect of a previous treatment to diminish. Vehicle for the PIO study was normal saline. For all other drugs, 10% DMSO in saline was administered to the mice with TIC injury to serve as the vehicle. One experimenter was blinded to the drugs given to the animals for each experiment.

### Statistical Analysis

Data were expressed as means  $\pm$  S.E.M. The GraphPad Prism 6 statistical program was used for data analyses (Graph Pad Software, Inc., La Jolla, CA). All behavioral data including drug studies were analyzed using a Two-Way ANOVA with a Fisher’s post hoc test; Histological studies were analyzed by a Two-Way ANOVA with a Tukey post hoc test; (where is appropriate)  $p < 0.05$  is considered significant.

## Results

### Mice with TIC Injury Displayed Unilateral Whisker Pad Mechanical Allodynia

The baseline mechanical threshold was initially the same on both sides of the whisker pad of mice with/without TIC ( $3.51 \pm 0.18$  g for the left;  $3.74 \pm 0.45$  g for the right). Mice with TIC injury experienced unilateral decreased mechanical threshold – an index of mechanical allodynia on the whisker pad ipsilateral to the surgery site within one week post-surgery lasting until the euthanasia day (week 14 post-injury). The mean 50% mechanical threshold of the ipsilateral whisker pad for the mice with TIC injury ( $0.24 \pm 0.92$  g) was significantly lower compared to that on the contralateral whisker pad ( $3.51 \pm 0.18$  g;  $n=8$ ;  $p<0.0001$ , two-way ANOVA, Fisher’s post hoc test, Figure 1). Also, the sham operation control mice did not demonstrate any changes in their mechanical threshold after surgery and were significantly different from whisker pad sensitivity associated with TIC nerve injury ( $3.51 \pm 0.36$  g vs.  $0.24 \pm 0.92$  g;  $n=8$ ;  $p<0.0001$ , two-way ANOVA, Fisher’s post hoc test).



## Effect of PPAR Agonists on Mechanical Allodynia of Mice with TIC Injury

**PPAR $\gamma$  Agonist, Pioglitazone, Attenuated Mechanical Allodynia in Mice with TIC Injury**—At 8 weeks post TIC, pioglitazone (300 mg/kg i.p.) effectively attenuated mechanical allodynia of the ipsilateral whisker pad. The mechanical threshold increased from  $0.24 \pm 0.092$  g before drug treatment to  $1.61 \pm 0.54$  g at hour 1, peaked at 2 hours ( $2.72 \pm 0.74$  g), and persisted for 3 hours ( $2.33 \pm 0.98$  g; Figure 2A). This was a significant increase in the threshold compared to the vehicle treated mice with TIC nerve injury ( $2.72 \pm 0.74$  g vs  $0.10 \pm 0.04$  g; two-way ANOVA, Fisher's post hoc test, \*\*\*\* $p < 0.0001$ ;  $n = 3-7$ ). Oral administration of pioglitazone hydrochloride (600 mg/kg p.o.) also attenuated mechanical allodynia in the mice with TIC injury (5 hr:  $0.87 \pm 0.32$  g; 6 hr:  $0.92 \pm 0.45$  g; two-way ANOVA, Fisher's post hoc test, \* $p < 0.05$ ;  $n = 3-7$ ) compared to the saline treated mice with TIC injury ( $0.03 \pm 0.00$  g; two-way ANOVA, Fisher's post hoc test, \* $p < 0.05$ ;  $n = 3-7$ ). This effect was significantly different at 5 and 6 hours post treatment. However, this dose was not as effective as the 300 mg/kg i.p. dose of pioglitazone. The 100 mg/kg i.p. dose of pioglitazone did not have an analgesic effect on the mice with TIC injury compared to saline treated mice ( $0.56 \pm 1.40$  g vs  $0.10 \pm 0.04$  g). The 300 mg/kg i.p. dose elicited hypothermic side effects that were most likely an indication that the dose was too high. However, the 100 mg/kg intraperitoneal injection and 600 mg/kg oral doses did not elicit any observable overt side effects. These results suggest that PPAR $\gamma$  receptor is a key player in whisker pad mechanical allodynia in the mice with TIC injury.

**PPAR $\beta/\delta$  Agonist Moderately Attenuated Mechanical Allodynia in the Mice with TIC Injury**—The administration of PPAR $\beta/\delta$  agonist, GW0742 (6 mg/kg i.p.), partially attenuated mechanical allodynia in mice with TIC injury compared to vehicle treated mice with TIC injury. The effect peaked at 2 hours post injection ( $1.59 \pm 0.55$  g vs.  $0.06 \pm 0.02$  g; two-way ANOVA, Fisher's post hoc test; \*\*\*\* $p < 0.0001$ ,  $n = 4-6$ ; Figure 2B). Administration of GW0742 1 mg/kg dose did not attenuate the mechanical allodynia ( $0.51 \pm 1.31$  g).

**PPAR $\alpha$  Agonist Had No Effect on the Mechanical Allodynia of Mice with TIC Injury**—Two PPAR $\alpha$  agonists were used in this experiment. Bezafibrate is a pan-PPAR agonist with the highest affinity for the alpha subunit. Bezafibrate at 100 mg/kg i.p. injection had no effect on mechanical allodynia in mice with TIC injury (treated:  $0.55 \pm 1.34$  g vs. vehicle:  $0.71 \pm 1.52$  g; two-way ANOVA, Fisher's post hoc test;  $p > 0.05$ ,  $n = 3-6$ ; Figure 2C). The second and more specific PPAR $\alpha$  agonist, fenofibrate, was administered at 200 mg/kg i.p. with attenuation on mechanical allodynia ( $0.56 \pm 1.28$  g) not observed at this particular dose. These results demonstrated that activation of PPAR $\alpha$  at these doses does not contribute to the attenuation of the mechanical allodynia in the mice with TIC injury.

**PPAR $\gamma$  Antagonist, GW9662, Blocked Analgesic Effects of Pioglitazone**—GW9662, a potent antagonist of PPAR $\gamma$ , at the dose of 30 mg/kg (i.p.) successfully blocked the actions of pioglitazone (300 mg/kg i.p.) in alleviating mechanical allodynia in mice with TIC injury (GW9662+PIO:  $0.53 \pm 1.29$  g vs. PIO only:  $1.55 \pm 1.41$  g; two-way ANOVA, Fisher's post hoc test,  $N = 4-7$ ; \*\*\*\* $p < 0.0001$ , Figure 2D). These results provide evidence

that PIO is acting through a PPAR $\gamma$  dependent mechanism to attenuate mechanical allodynia.

**Increased PPAR $\gamma$  Immunoreactivity in spV of Mice with TIC injury**—The entire trigeminal brainstem sensory spV nucleus was analyzed for PPAR $\gamma$  immunoreactivity (mean intensities) in mice three weeks after TIC injury for comparison with naïve controls. Although the PPAR $\gamma$  positive neurons were stained in both mice with TIC and naïve mice, the PPAR $\gamma$ -like immunoreactivity greatly increased in specific regions of the spV nucleus in the injured animals. Figure 3A shows the tissue sections through the entire spV in a naïve mouse and in a mouse with TIC nerve injury. Higher power micrographs of tissue sections representing each level of the spV from a mouse with TIC nerve injury provide detail within spV at each level Figure 3B–E.

Figure 4 depicts the mean intensities of the immunoreactivity of PPAR $\gamma$  throughout the spV in the mice with TIC injury compared to naïve mice (n=3 with 9–12 sections/animal). There was significantly higher relative optical density for PPAR $\gamma$  immunoreactivity in the spV of the mice with TIC nerve injury. That is, densitometry of PPAR $\gamma$  immunostaining in the spV rostral ( $85.65 \pm 19.37$ ) and caudal ( $65.43 \pm 12.68$ ) oralis. Subnucleus caudalis on the ipsilateral side of TIC nerve injury, including densitometry of PPAR $\gamma$  immunostaining in the spV revealed the highest intensity in mice with TIC injury ( $93.59 \pm 27.62$ ) compared to naïve mice (rostral oralis:  $67.21 \pm 14.01$ ; caudal oralis:  $46.42 \pm 18.46$ ; caudalis:  $71.76 \pm 17.31$ ;  $p < 0.05$ ; two-way ANOVA, Fisher's post hoc test). Immunostaining intensity in the spinal trigeminal interpolaris of the mice with TIC injury ( $75.61 \pm 17.48$ ) was not significantly different from naïve mice ( $65.64 \pm 15.78$ ). However, PPAR $\gamma$  immunoreactivity in the spinal trigeminal caudalis of the mice with TIC injury was greater than that of the other trigeminal spinal subnuclei and significantly different from oralis ( $p < 0.01$ ) and interpolaris ( $p < 0.05$ ; two-way ANOVA, Fisher's post hoc, n=3 with 9–12 sections/animal). Furthermore, there was a bilateral increase in PPAR $\gamma$  immunoreactivity only in the spV caudal oralis in mice with TIC injury (ipsilateral:  $65.43 \pm 12.68$ , contralateral:  $67.22 \pm 10.89$ ).

Figure 5 illustrates the ipsilateral spinal trigeminal interpolaris in the mice with TIC injury compared to naïve mice. Although PPAR $\gamma$  immunoreactivity also appears in the spV of naïve mice (**A, B**), the mean staining intensity was much less compared to that of the mice with TIC nerve injury (**C, D**). The white arrows indicate the nerve axonal projections of whisker barrels of spinal trigeminal zone that have been shown to correlate with the receptive fields on the whisker pads of the mice<sup>43</sup>. As indicated in this 20 $\times$  image, PPAR $\gamma$  positive neurons were primarily located at the sites indicated by the black arrows. PPAR $\gamma$  also appears to be localized in very small nuclei consistent with previous findings of PPAR $\gamma$  staining in glial nuclei<sup>6, 24, 29</sup>.

## Discussion

This study determined that PPAR $\gamma$  plays a significant role in trigeminal mechanical sensitivity testing. Histological images revealed that 3 weeks after TIC nerve injury intense PPAR $\gamma$  immunoreactivity appeared in the spV caudalis compared to other subnuclei of the



brainstem trigeminal dorsal horn where the primary nociceptive nerve fibers synapse onto second order neurons. Systemic administration of a PPAR $\gamma$  agonist, PIO, attenuated the mechanical allodynia in mice with TIC nerve injury at doses of 300 mg/kg i.p. and 600 mg/kg p.o. The higher efficacy of the 300 versus the 600 mg/kg dose is likely reflective of decreased bioactivity after gastric degradation. Differences in drug effect on pain related behavior in the current study was reflective of the different routes of administration utilized. The LD50s for all drugs are shown in Table 1. Administration of a PPAR $\gamma$  antagonist, GW9662 (30 mg/kg i.p.) prior to the optimal dose of PIO (300 mg/kg i.p.) blocked the analgesic effect of PIO indicating that PIO is acting through a PPAR $\gamma$  mechanism. Taken together, these results confirm PPAR $\gamma$ 's role in trigeminal pain transmission. Upon PPAR $\gamma$  activation, reduced inflammation and reduction of neuropathic pain after an injury has also been reported that would also contribute to reduced pain related behavior<sup>6, 15, 25-28</sup>.

PPAR $\gamma$  has been more thoroughly investigated than PPAR $\beta/\delta$ . Only a limited number of other studies have reported that PPAR $\beta/\delta$  agonists attenuate inflammatory pain<sup>44, 45</sup>. The biological role of PPAR $\beta/\delta$  has remained elusive due, in part, to its broad tissue expression and the lack of good chemical tools with which to study its physiological function. However, the PPAR $\beta/\delta$  agonist, GW0742 had a minimal attenuation effect on the allodynia in the mice with TIC injury. The results showed that activation of PPAR $\beta/\delta$  isoform may play some role in the mechanical allodynia induced by the TIC nerve injury, but additional doses should be tested.

Based on the findings here, PPAR $\gamma$  and PPAR $\beta/\delta$  are potential therapeutic targets to inhibit transmission of pain, whereas PPAR $\alpha$  does not appear to be a key player in trigeminal neuropathic pain. This is in contrast to a few controversial studies reporting PPAR $\alpha$  activation has an inhibitory effect on nociception after nerve injury or inflammation<sup>6, 36, 46, 47</sup>. No study has reported PPAR $\alpha$  activation eliciting an analgesic effect in trigeminal neuropathic pain. Likewise, the PPAR $\alpha$  agonists, bezafibrate and fenofibrate, had no effect on the allodynia in the present studies. However, use of higher doses of the two PPAR $\alpha$  agonists may have increased the possibility of providing an analgesic effect in the mice with TIC injury.

It is well known that PPAR isoforms are widely expressed in adipose, liver, cardiac, endometrial stromal cells, immune cells, neurons, and glia of the peripheral and central nervous system<sup>9-17</sup>. Therefore, systemic administration of PIO will affect all PPAR $\gamma$  receptors. In this paper, we wanted to show PPAR $\gamma$ 's presence in the trigeminal pain transmission pathway, specifically the trigeminal spinal nucleus caudalis, as this was the most likely site of action in reducing the hypersensitivity in the whisker pad region caused by the TIC surgery.

Moreno and colleagues previously reported PPAR $\gamma$  in the dorsal horn of the brainstem and spinal cord<sup>32</sup>. Maedo and colleagues confirmed Moreno's findings as well as described localization in the sciatic nerve, dorsal root ganglia, and dorsal horn<sup>48</sup>. These findings supported a role for PPAR $\gamma$  in the somatic nociceptive pathway.

The present study revealed that PPAR $\gamma$  immunoreactivity increases three weeks after the TIC nerve injury. This is consistent with the findings that PPAR $\gamma$  is upregulated within weeks after other nerve injuries<sup>29, 31</sup>. Additionally, our findings support previous studies demonstrating PPAR $\gamma$ 's presence in neuronal and glial cells<sup>6</sup>. Although this study identified PPAR $\gamma$  immunoreactivity in putative neurons, future double-labeling experiments in spV with PPAR $\gamma$ , neuronal, and glial markers (neuN, IB-4, OX-42) would serve as more conclusive evidence of PPAR $\gamma$ 's presence in neurons and/or glial cells, supporting its role in neurogenic inflammation.

PPAR $\gamma$  activation has been shown to transrepress NF- $\kappa$ B thereby downregulating pro-inflammatory cytokines such as IL-6 and TNF- $\alpha$ <sup>6-8, 24, 49</sup>. Previous studies have reported that PPAR $\gamma$  deficient mice are more vulnerable to inflammatory diseases<sup>50-52</sup>. In our previous study<sup>35</sup>, we demonstrated microglial activation in the trigeminal dorsal horn of mice with TIC nerve injury. Therefore, one possible reason for the increase in PPAR $\gamma$  immunoreactivity observed in the mice with TIC injury could be the inflammatory response occurring in the trigeminal dorsal horn. The upregulation of PPAR $\gamma$  in the trigeminal nuclei likely indicates PPAR $\gamma$  is activated to diminish the effects of the neuroglial immune system to counter or downregulate the pro-inflammatory cytokines.

Interestingly, PPAR $\gamma$  immunoreactivity was most intense in the spV caudalis of the mice with TIC injury while barely detectable in naïve mice. Since the spV caudalis has been identified as the primary nucleus for transmission of nociceptive signaling<sup>3, 33, 53, 54</sup>, the increased expression might indicate why the PPAR $\gamma$  receptor agonist, PIO, has analgesic effects on mechanical allodynia in mice with TIC injury. With the upregulation of PPAR $\gamma$ , a stronger anti-inflammatory cell signaling effect could be initiated once PIO binds to its receptor.

However, there is much debate about the actions of PIO. Some scholars believe that PIO activates PPAR $\gamma$  to induce transcription while others believe there are PPAR $\gamma$  transcription independent mechanisms occur to decrease allodynia<sup>6, 25, 38, 42, 55</sup>. Still, others suspect and have possibly demonstrated that PIO can act on other intracellular receptors such as acting on a mitochondrial membrane protein known as mitoNEET<sup>56</sup>. This would decrease cellular oxidative stress, a known initiator of chronic pain<sup>57</sup>. However, in present study, the block of PIO's analgesic actions by the PPAR $\gamma$  antagonist, GW9662, leads us to suggest that PIO attenuates trigeminal nociception at least in part by acting through PPAR $\gamma$  signaling. More studies need to be conducted to elucidate the action of PIO non-PPAR $\gamma$  dependent pathways.

## Conclusion

Overall this novel study determined that PPAR $\gamma$  activation by PIO is a potential therapeutic target for treatment of orofacial neuropathic pain. The present study was not only the first to demonstrate that PPAR $\gamma$  activation attenuates hypersensitivity induced in a trigeminal neuropathic pain model, but this is also the first study to identify PPAR $\gamma$  immunoreactivity throughout the trigeminal brainstem sensory nucleus which increases after trigeminal nerve

injury. Taken together, these studies provide information relevant to utilization of PIO as a potential treatment for patients suffering from orofacial neuropathic pain.

## Acknowledgments

The authors wish to thank Dr. Tracey Kniffin for behavioral testing assistance, and Dr. Charles Carlson for knowledgeable discussions. These studies were funded by NIH COBRE 2P20RR020145 (Ebersole), NIH NINDS R01039041 (KNW), and an institutional Wethington Award (KNW).

## References

1. Zakrzewska JM. Differential diagnosis of facial pain and guidelines for management. *Br J Anaesth*. 2013; 111:95–104. [PubMed: 23794651]
2. Asmundson GJ, Katz J. Understanding the co-occurrence of anxiety disorders and chronic pain: state-of-the-art. *Depress Anxiety*. 2009; 26:888–901. [PubMed: 19691031]
3. De Leeuw, R. Orofacial Pain: Guidelines for Assessment, Diagnosis, and Management. 4. Hanover Park, IL: Quintessence Publishing Co, Inc; 2008. p. 316
4. Robinson MJ, Edwards SE, Iyengar S, Bymaster F, Clark M, Katon W. Depression and pain. *Front Biosci (Landmark Ed)*. 2009; 14:5031–51. [PubMed: 19482603]
5. Roditi D, Robinson ME, Litwins N. Effects of coping statements on experimental pain in chronic pain patients. *J Pain Res*. 2009; 2:109–16. [PubMed: 21197299]
6. Maeda T, Kishioka S. PPAR and Pain. *Int Rev Neurobiol*. 2009; 85:165–77. [PubMed: 19607969]
7. Combs CK, Johnson DE, Karlo JC, Cannady SB, Landreth GE. Inflammatory mechanisms in Alzheimer's disease: inhibition of beta-amyloid-stimulated proinflammatory responses and neurotoxicity by PPARgamma agonists. *J Neurosci*. 2000; 20:558–67. [PubMed: 10632585]
8. Berger J, Moller DE. The mechanisms of action of PPARs. *Annu Rev Med*. 2002; 53:409–35. [PubMed: 11818483]
9. Cimini A, Cristiano L, Colafarina S, et al. PPARgamma-dependent effects of conjugated linoleic acid on the human glioblastoma cell line (ADF). *Int J Cancer*. 2005; 117:923–33. [PubMed: 15986437]
10. Cimini A, Benedetti E, Cristiano L, et al. Expression of peroxisome proliferator-activated receptors (PPARs) and retinoic acid receptors (RXRs) in rat cortical neurons. *Neuroscience*. 2005; 130:325–37. [PubMed: 15664689]
11. Cristiano L, Cimini A, Moreno S, Ragnelli AM, Paola Ceru M. Peroxisome proliferator-activated receptors (PPARs) and related transcription factors in differentiating astrocyte cultures. *Neuroscience*. 2005; 131:577–87. [PubMed: 15730864]
12. Cullingford TE, Dolphin CT, Sato H. The peroxisome proliferator-activated receptor alpha-selective activator ciprofibrate upregulates expression of genes encoding fatty acid oxidation and ketogenesis enzymes in rat brain. *Neuropharmacology*. 2002; 42:724–30. [PubMed: 11985831]
13. Gray E, Ginty M, Kemp K, Scolding N, Wilkins A. The PPAR-gamma agonist pioglitazone protects cortical neurons from inflammatory mediators via improvement in peroxisomal function. *J Neuroinflammation*. 2012; 9:63. [PubMed: 22480361]
14. Li W, He X, Shi W, Jia H, Zhong B. Pan-PPAR agonists based on the resveratrol scaffold: biological evaluation and docking studies. *ChemMedChem*. 2010; 5:1977–82. [PubMed: 20973122]
15. Park SW, Yi JH, Miranpuri G, et al. Thiazolidinedione class of peroxisome proliferator-activated receptor gamma agonists prevents neuronal damage, motor dysfunction, myelin loss, neuropathic pain, and inflammation after spinal cord injury in adult rats. *J Pharmacol Exp Ther*. 2007; 320:1002–12. [PubMed: 17167171]
16. Sarruf DA, Yu F, Nguyen HT, et al. Expression of peroxisome proliferator-activated receptor-gamma in key neuronal subsets regulating glucose metabolism and energy homeostasis. *Endocrinology*. 2009; 150:707–12. [PubMed: 18845632]

17. McKinnon B, Bersinger NA, Mueller MD. Peroxisome proliferating activating receptor gamma-independent attenuation of interleukin 6 and interleukin 8 secretion from primary endometrial stromal cells by thiazolidinediones. *Fertil Steril*. 2012; 97:657–64. [PubMed: 22192353]
18. Michalik L, Wahli W. Involvement of PPAR nuclear receptors in tissue injury and wound repair. *J Clin Invest*. 2006; 116:598–606. [PubMed: 16511592]
19. Szanto A, Narkar V, Shen Q, Uray IP, Davies PJ, Nagy L. Retinoid X receptors: X-ploring their (patho)physiological functions. *Cell Death Differ*. 2004; 11(Suppl 2):S126–43. [PubMed: 15608692]
20. Sanz MJ, Albertos F, Otero E, Juez M, Morcillo EJ, Piqueras L. Retinoid X receptor agonists impair arterial mononuclear cell recruitment through peroxisome proliferator-activated receptor-gamma activation. *J Immunol*. 2012; 189:411–24. [PubMed: 22661092]
21. Moore KJ, Rosen ED, Fitzgerald ML, et al. The role of PPAR-gamma in macrophage differentiation and cholesterol uptake. *Nat Med*. 2001; 7:41–7. [PubMed: 11135614]
22. Willson TM, Lambert MH, Kliewer SA. Peroxisome proliferator-activated receptor gamma and metabolic disease. *Annu Rev Biochem*. 2001; 70:341–67. [PubMed: 11395411]
23. Nagashima K, Lopez C, Donovan D, et al. Effects of the PPARgamma agonist pioglitazone on lipoprotein metabolism in patients with type 2 diabetes mellitus. *J Clin Invest*. 2005; 115:1323–32. [PubMed: 15841215]
24. Sadeghian M, Marinova-Mutafchieva L, Broom L, et al. Full and partial peroxisome proliferation-activated receptor-gamma agonists, but not delta agonist, rescue of dopaminergic neurons in the 6-OHDA parkinsonian model is associated with inhibition of microglial activation and MMP expression. *J Neuroimmunol*. 2012; 246:69–77. [PubMed: 22498097]
25. Fehrenbacher JC, Loverme J, Clarke W, Hargreaves KM, Piomelli D, Taylor BK. Rapid pain modulation with nuclear receptor ligands. *Brain Res Rev*. 2009; 60:114–24. [PubMed: 19162071]
26. Ghosh S, Patel N, Rahn D, et al. The thiazolidinedione pioglitazone alters mitochondrial function in human neuron-like cells. *Mol Pharmacol*. 2007; 71:1695–702. [PubMed: 17387142]
27. Morgenweck J, Griggs RB, Donahue RR, Zadina JE, Taylor BK. PPARgamma activation blocks development and reduces established neuropathic pain in rats. *Neuropharmacology*. 2013; 70:236–46. [PubMed: 23415633]
28. Morgenweck J, Abdel-Aleem OS, McNamara KC, Donahue RR, Badr MZ, Taylor BK. Activation of peroxisome proliferator-activated receptor gamma in brain inhibits inflammatory pain, dorsal horn expression of Fos, and local edema. *Neuropharmacology*. 2010; 58:337–45. [PubMed: 19891980]
29. Cao Y, Wang Q, Zhou Z, et al. Changes of peroxisome proliferator-activated receptor-gamma on crushed rat sciatic nerves and differentiated primary Schwann cells. *J Mol Neurosci*. 2012; 47:380–8. [PubMed: 22094441]
30. Zhang F, Liu F, Yan M, et al. Peroxisome proliferator-activated receptor-gamma agonists suppress iNOS expression induced by LPS in rat primary Schwann cells. *J Neuroimmunol*. 2010; 218:36–47. [PubMed: 19942298]
31. Zhu J, Zhang J, Ji M, et al. The role of peroxisome proliferator-activated receptor and effects of its agonist, pioglitazone, on a rat model of optic nerve crush: PPARgamma in retinal neuroprotection. *PLoS One*. 2013; 8:e68935. [PubMed: 23874818]
32. Moreno S, Farioli-Vecchioli S, Ceru MP. Immunolocalization of peroxisome proliferator-activated receptors and retinoid X receptors in the adult rat CNS. *Neuroscience*. 2004; 123:131–45. [PubMed: 14667448]
33. Sessle BJ. Acute and chronic craniofacial pain: brainstem mechanisms of nociceptive transmission and neuroplasticity, and their clinical correlates. *Crit Rev Oral Biol Med*. 2000; 11:57–91. [PubMed: 10682901]
34. DaSilva AF, DosSantos MF. The role of sensory fiber demography in trigeminal and postherpetic neuralgias. *J Dent Res*. 2012; 91:17–24. [PubMed: 21670221]
35. Ma F, Zhang L, Lyons D, Westlund KN. Orofacial neuropathic pain mouse model induced by Trigeminal Inflammatory Compression (TIC) of the infraorbital nerve. *Mol Brain*. 2012; 5:44. [PubMed: 23270529]

36. Oliveira AC, Bertollo CM, Rocha LT, Nascimento EB Jr, Costa KA, Coelho MM. Antinociceptive and antiedematogenic activities of fenofibrate, an agonist of PPAR alpha, and pioglitazone, an agonist of PPAR gamma. *European journal of pharmacology*. 2007; 561:194–201. [PubMed: 17343847]
37. Gross V, Schneider W, Schunck WH, Mervaala E, Luft FC. Chronic effects of lovastatin and bezafibrate on cortical and medullary hemodynamics in deoxycorticosterone acetate-salt hypertensive mice. *Journal of the American Society of Nephrology: JASN*. 1999; 10:1430–9. [PubMed: 10405198]
38. Feinstein DL, Spagnolo A, Akar C, et al. Receptor-independent actions of PPAR thiazolidinedione agonists: is mitochondrial function the key? *Biochem Pharmacol*. 2005; 70:177–88. [PubMed: 15925327]
39. Hamano Y, Okude T, Yokosuka O, Ogawa M. Attenuation of Immune-Mediated Renal Injury by Telmisartan, an Angiotensin Receptor Blocker and a Selective PPAR-gamma Activator. *Nephron extra*. 2011; 1:78–90. [PubMed: 22470382]
40. Paterniti I, Mazzon E, Riccardi L, et al. Peroxisome proliferator-activated receptor beta/delta agonist GW0742 ameliorates cerulein- and taurocholate-induced acute pancreatitis in mice. *Surgery*. 2012; 152:90–106. [PubMed: 22521259]
41. Turner PV, Brabb T, Pekow C, Vasbinder MA. Administration of substances to laboratory animals: routes of administration and factors to consider. *Journal of the American Association for Laboratory Animal Science: JAALAS*. 2011; 50:600–13. [PubMed: 22330705]
42. Lea MA, Sura M, Desbordes C. Inhibition of cell proliferation by potential peroxisome proliferator-activated receptor (PPAR) gamma agonists and antagonists. *Anticancer Res*. 2004; 24:2765–71. [PubMed: 15517883]
43. Zembrzycki A, Chou SJ, Ashery-Padan R, Stoykova A, O’Leary DD. Sensory cortex limits cortical maps and drives top-down plasticity in thalamocortical circuits. *Nat Neurosci*. 2013; 16:1060–7. [PubMed: 23831966]
44. Gill N, Bijjem KR, Sharma PL. Anti-inflammatory and anti-hyperalgesic effect of all-trans retinoic acid in carrageenan-induced paw edema in Wistar rats: involvement of peroxisome proliferator-activated receptor-beta/delta receptors. *Indian J Pharmacol*. 2013; 45:278–82. [PubMed: 23833373]
45. Hall MG, Quignodon L, Desvergne B. Peroxisome Proliferator-Activated Receptor beta/delta in the Brain: Facts and Hypothesis. *PPAR Res*. 2008; 2008:780452. [PubMed: 19009042]
46. LoVerme J, Russo R, La Rana G, et al. Rapid broad-spectrum analgesia through activation of peroxisome proliferator-activated receptor-alpha. *J Pharmacol Exp Ther*. 2006; 319:1051–61. [PubMed: 16997973]
47. Benani A, Heurtaux T, Netter P, Minn A. Activation of peroxisome proliferator-activated receptor alpha in rat spinal cord after peripheral noxious stimulation. *Neurosci Lett*. 2004; 369:59–63. [PubMed: 15380308]
48. Maeda A, Horikoshi S, Gohda T, Tsuge T, Maeda K, Tomino Y. Pioglitazone attenuates TGF-beta(1)-induction of fibronectin synthesis and its splicing variant in human mesangial cells via activation of peroxisome proliferator-activated receptor (PPAR)gamma. *Cell Biol Int*. 2005; 29:422–8. [PubMed: 16054559]
49. Scholz J, Woolf CJ. The neuropathic pain triad: neurons, immune cells and glia. *Nat Neurosci*. 2007; 10:1361–8. [PubMed: 17965656]
50. Adachi M, Kurotani R, Morimura K, et al. Peroxisome proliferator activated receptor gamma in colonic epithelial cells protects against experimental inflammatory bowel disease. *Gut*. 2006; 55:1104–13. [PubMed: 16547072]
51. Straus DS, Glass CK. Anti-inflammatory actions of PPAR ligands: new insights on cellular and molecular mechanisms. *Trends Immunol*. 2007; 28:551–8. [PubMed: 17981503]
52. Cuzzocrea S, Pisano B, Dugo L, et al. Rosiglitazone, a ligand of the peroxisome proliferator-activated receptor-gamma, reduces acute inflammation. *European journal of pharmacology*. 2004; 483:79–93. [PubMed: 14709329]

53. Coimbra F, Coimbra A. Dental noxious input reaches the subnucleus caudalis of the trigeminal complex in the rat, as shown by c-fos expression upon thermal or mechanical stimulation. *Neurosci Lett*. 1994; 173:201–4. [PubMed: 7936415]
54. Dubner R, Ren K. Brainstem mechanisms of persistent pain following injury. *Journal of orofacial pain*. 2004; 18:299–305. [PubMed: 15636012]
55. Thal SC, Heinemann M, Luh C, Pieter D, Werner C, Engelhard K. Pioglitazone reduces secondary brain damage after experimental brain trauma by PPAR-gamma-independent mechanisms. *J Neurotrauma*. 2011; 28:983–93. [PubMed: 21501066]
56. Yonutas HM, Sullivan PG. Targeting PPAR isoforms following CNS injury. *Curr Drug Targets*. 2013; 14:733–42. [PubMed: 23627890]
57. Trevisan G, Benemei S, Materazzi S, et al. TRPA1 mediates trigeminal neuropathic pain in mice downstream of monocytes/macrophages and oxidative stress. *Brain: a journal of neurology*. 2016; 139:1361–77. [PubMed: 26984186]



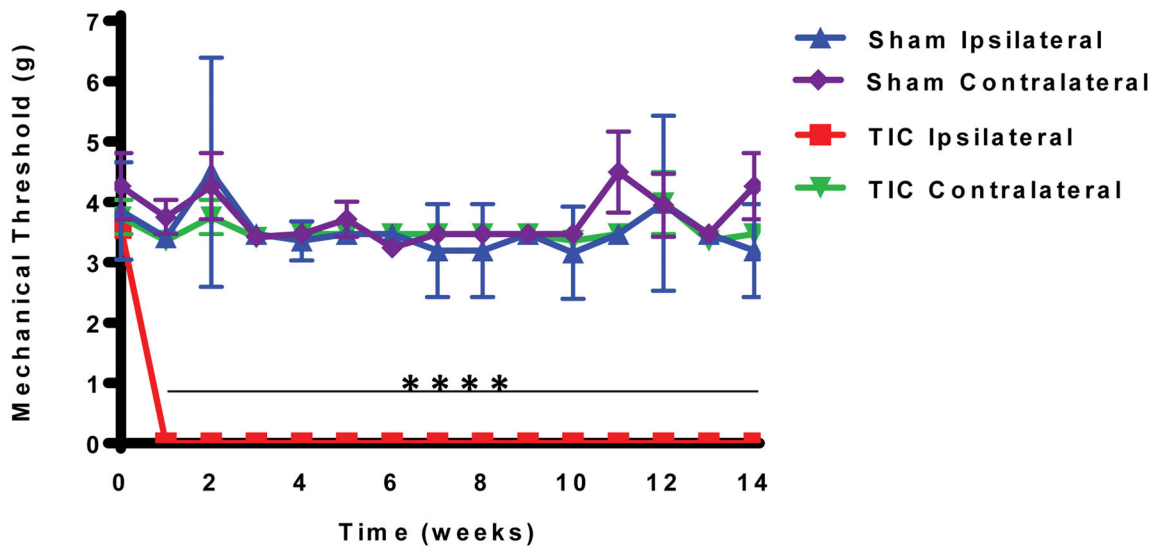


**Figure 1. Mice with TIC Injury Developed Persistent Unilateral Mechanical Allodynia on the Ipsilateral Whisker Pad**

The 50% mechanical threshold on whisker pads of the mice with TIC injury and the sham mice were measured bilaterally for detecting mechanical allodynia. The mechanical threshold on the ipsilateral whisker pad of mice with TIC injury was significantly decreased within one week of injury and remained decreased until euthanasia, week 14 (indicated with thin black line). The mechanical threshold on contralateral whisker pad of the mice with TIC injury was unaffected by the surgery. The mechanical threshold on the whisker pads of the sham operation mice did not change. (n=8/group; \*\*\*\* $p < 0.0001$ , two-way ANOVA, Fisher's post hoc test)

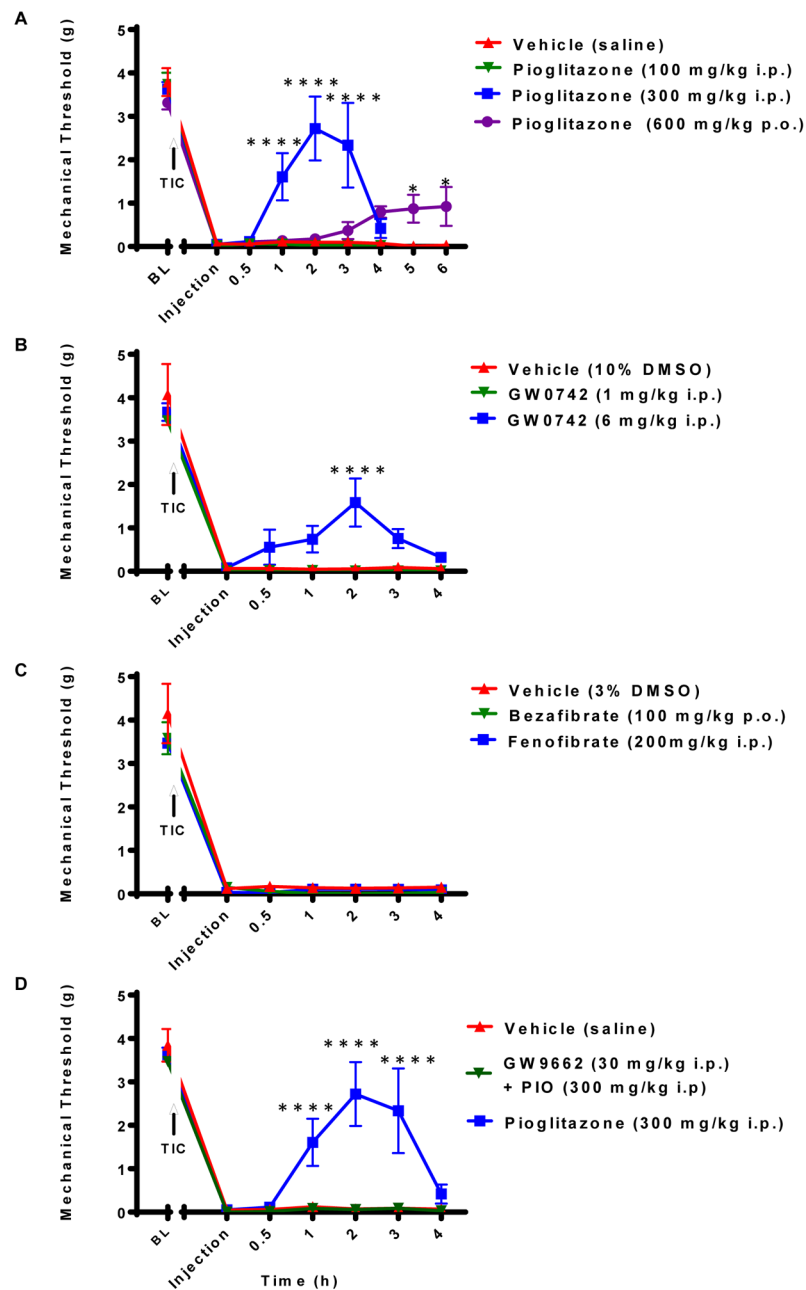


**Figure 2. PIO Attenuated Whisker Pad Mechanical Allodynia in the Mice with TIC Injury**  
 Hypersensitivity was attenuated by specific PPAR $\gamma$  agonism with (A) PIO rapidly elevating the 50% mechanical threshold in the mice with TIC at higher doses (300 mg/kg and 600 mg/kg), but was ineffective at 100 mg/kg (n=3–7). (B) GW0742, PPAR $\beta$  agonist, attenuated mechanical allodynia in the mice with TIC injury at a dose of 6 mg/kg, but was not as effective as PIO (n=4–6). (C) PPAR $\alpha$  agonists, Bezafibrate and fenofibrate at indicated doses, were not effective in alleviating mechanical allodynia in the mice with TIC injury (n=3–6). (D) PPAR $\gamma$  antagonist, GW9662, blocked the anti-allodynic effect of PIO at a dose of 30 mg/kg (n=4–7). (\* $p$ <0.05, \*\*\*\* $p$ <0.0001; two-way ANOVA, Fisher's post hoc test)

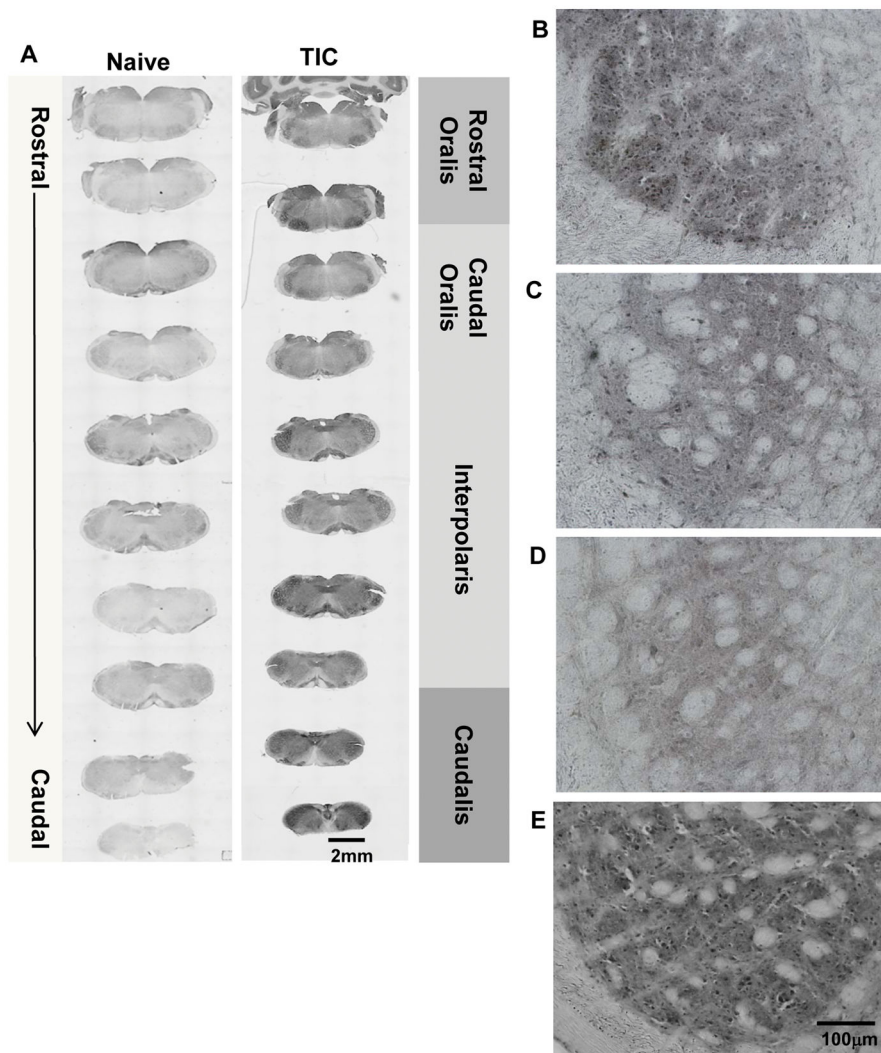


### Figure 3. PPAR $\gamma$ Localization Throughout SpV of Mice with TIC Injury

(A) The photomicrographic images depict the rostral to caudal distribution of PPAR $\gamma$  in the spV nucleus of naïve and TIC injured mice. PPAR $\gamma$  is localized throughout most of the spV in TIC injured mice and is more abundant than in naïve mice. The low power images show intensity differences in PPAR $\gamma$  among individual spV subnuclei (rostral and caudal oralis, interpolaris, caudalis). Density differences are seen in the rostral (B) versus caudal (C) oralis subnuclei in mice with TIC injury. (D) Less density for PPAR $\gamma$  is localized in spV subnucleus interpolaris in mice with TIC injury. (E) Dense localization of PPAR $\gamma$  is evident in spV caudalis subnucleus in mice with TIC injury.

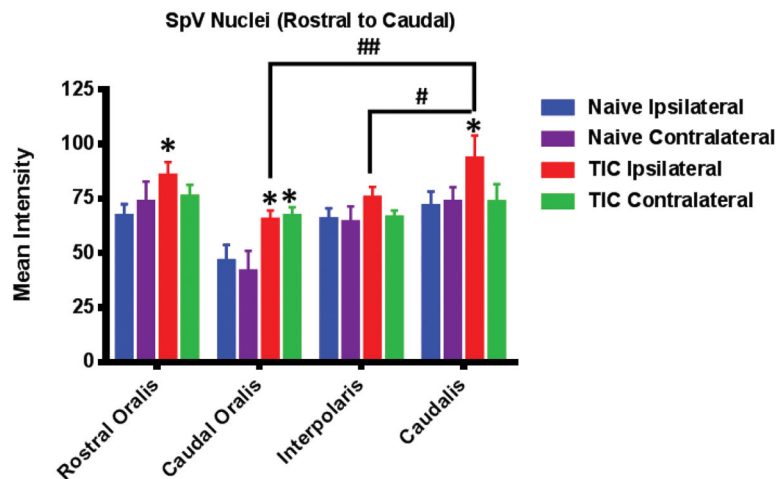


#### Figure 4. PPAR $\gamma$ Immunoreactivity Increased in spV of Mice with TIC Injury

The mice with TIC injury had an increased PPAR $\gamma$  immunoreactivity in the ipsilateral spV rostral oralis and subnucleus caudalis compared to naïve mice (n=3 with 9–12 sections/animal) (\* $p$ <0.05, two-way ANOVA, Fisher's post hoc). Mean intensity of immunofluorescence is shown along the Y-axis. The spV caudal oralis subnucleus expressed bilateral immunoreactivity that was significantly greater than tissue from naïve mice (\* $p$ <0.05, two-way ANOVA, Fisher's post hoc). PPAR $\gamma$  immunoreactivity was also significantly higher in ipsilateral spV caudalis in mice with TIC injury compared spV oralis and interpolaris. (# $p$ <0.05, ## $p$ <0.01, two-way ANOVA, Fisher's post hoc)

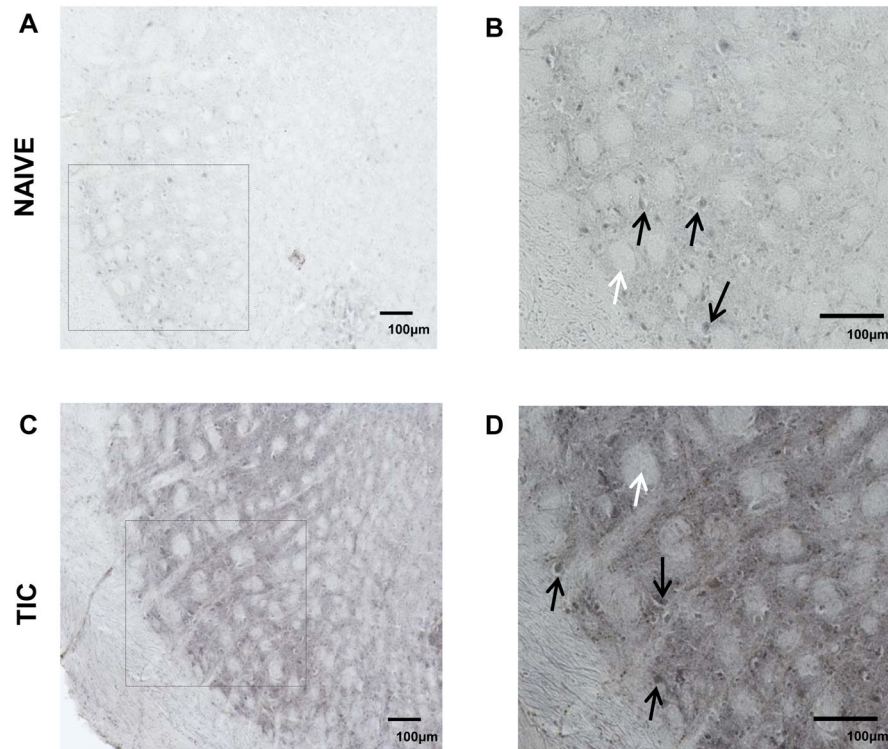


**Figure 5. PPAR $\gamma$  Immunoreactivity in SpV Interpolaris in Sham and TIC Injured Mice**  
The upper panels illustrate PPAR $\gamma$  in ipsilateral spV dorsal horn where most PPAR $\gamma$  positive cells were most apparent shown from sham mice at lower (A) and higher magnification (B). The lower panels (C) and (D) illustrate ipsilateral side PPAR $\gamma$  in mice with TIC injury. The black arrows indicate PPAR $\gamma$  positive cells and the white arrows indicate the whisker barrel axonal projections from the mouse whisker pad receptive fields. As shown by the pictures, the staining intensity of PPAR $\gamma$  immunoreactivity was more intense in the tissue sections from the TIC injured mice than from the sham mice.

**Table 1**Drug Information. PPAR $\gamma$  Agonists and Antagonists

<b>Drug</b>	<b>Actions</b>	<b>Dose</b>	<b>Administration</b>	<b>LD50</b>
<b>Pioglitazone</b>	PPAR $\gamma$ agonist	100 mg/kg	Intraperitoneal	181–1200 mg/kg
<b>Pioglitazone</b>	PPAR $\gamma$ agonist	300 mg/kg	Intraperitoneal	181–1200 mg/kg
<b>Pioglitazone</b>	PPAR $\gamma$ agonist	600 mg/kg	Oral	181–1200 mg/kg
<b>GW0742</b>	PPAR $\beta/\delta$ agonist	1 mg/kg	Intraperitoneal	Not reported
<b>GW0742</b>	PPAR $\beta/\delta$ agonist	6 mg/kg	Intraperitoneal	Not reported
<b>Bezafibrate</b>	PPAR $\alpha$ agonist	100 mg/kg	Oral	500 mg/kg
<b>Fenofibrate</b>	PPAR $\alpha$ agonist	200 mg/kg	Intraperitoneal	1200 mg/kg
<b>GW9662</b>	PPAR $\gamma$ antagonist	30 mg/kg	Intraperitoneal	Not reported

Author Manuscript

Author Manuscript

Author Manuscript

Author Manuscript